Semester Thesis

Extending RT-TDHF to Include Magnetic Field Interactions

Massimo Solinas

Spring Term 2024

Supervised by:
Dr. Andreas Adelmann

Author:
Massimo Solinas

Scientific advisor:
Sebastian Heinekamp
Raphael Husistein

Abstract

This project aims to enhance the Real-Time Time Dependent Hartree Fock (RT-TDHF) method by incorporating interactions with time-varying magnetic fields. Building on the work of R. Husistein, this research extends the simulation of the internal state to include Zeeman and hyperfine interactions, as well as spin-orbit coupling. To achieve this, a new Roothaan equation is derived to account for the effects of the updated Hamiltonian, integrating the nuclear spin degree of freedom into the total wavefunction and rewriting the new Fock operator.
The new implementation is tested through simulations of the Be^+ ion, demonstrating accurate hyperfine splitting and the spectrum behavior of the system under an external magnetic field, consistent with predictions from Breit-Rabi diagrams.

Contents

Introduction

Quantum computers represent a fundamental change in computing, taking advantage of the principles of quantum mechanics to revolutionize computation. Unlike classical computers, which use bits as units of information represented as either 0 or 1, quantum computers employ quantum bits or qubits. The main feature of qubits is their ability to exist in superposition, allowing them to represent both 0 and 1 simultaneously. This intrinsic property enables quantum computers to perform vast numbers of calculations in parallel, unlocking exponential increases in computational power compared to classical counterparts. Furthermore, quantum computers exploit the phenomenon of entanglement, for which qubits become correlated in such a way that the state of one qubit influences the state of another. This allows quantum computers to solve certain classes of problems with remarkable efficiency. However, the realization of practical quantum computers remains a challenge, requiring precise control over quantum states and the mitigation of decoherence, the phenomenon for which quantum systems become susceptible to errors due to interactions with their environment. The quest for quantum supremacy motivates researchers to find and study innovative architectures that can handle an increasing number of qubits. While the two prevailing approaches are based on trapped ions and superconducting circuits, Brown and Roser [1] proposed a novel methodology: employing storage rings as the underlying framework for quantum computation. Their innovative idea comes from realizing that storage rings and ion traps work in similar ways, using electric and magnetic fields to keep particles on specific paths. Ion traps hold particles still, while particles in storage rings move in circles.
Significant practical challenges stand in the way of making these ideas work in reality. One big challenge is figuring out new ways to cool ions to temperatures much colder than what is possible to do now. Since it is difficult to try these ideas out in experiments right away, simulations become crucial, since they might help to understand the underlying phenomenology.

R. Husistein showed in [2] a methodology to simulate the internal and external state separately and then a way to combining them to achieve the full system. His implementation uses the the Hagedorn wavefunctions to represent the external state, and adopts the Real-Time Time Dependent Hartree Fock method (RT-TDHF) to simulate the internal state also including the spin degree of freedom of the electrons. The aim of the the following project is to further extend the work done by R. Husistein in order to adapt the RT-TDHF method to include a time varying electromagnetic field, spin-orbit coupling and the hyperfine interaction, crucial to simulate and study the decoherence time of an ion trapped in a storage ring.

Chapter 1

Theoretical Concepts

To fully simulate the system composed of an ion moving in a storage ring, it is possible to break down the problem into two primary components: the external state and the internal state. This project primarily concentrates on the latter aspect. However, a concise theoretical overview of both systems will be provided. A more detailed explanation can be found in [2].

1.1 Internal State

The internal state represents the basic quantum mechanical two-level system essential for defining a qubit accurately. One of the simplest methods to establish such a system involves considering an ionized atom, composed by the nucleus along with all core and valence electrons. To simplify this setup, the nucleus is characterized by an effective core potential (ECP), meaning that the nucleus and the core electrons are effectively treated as a single entity with a modified potential, while valence electrons are treated explicitly. Finally, the two-level system is given by the hyperfine splitting, which arises from the coupling between the magnetic moments associated with the nuclear spin and the electronic spin. In the context of defining qubits, hyperfine splitting can be exploited to create well-defined energy states that serve as the basis for qubit operations. By manipulating the splitting through external fields, such as magnetic fields, one can control the transitions between these energy levels.
Focusing on ions which posses a single valence electron, such as $^9Be^+$, it is possible to write the Hamiltonian in the following way:

$$H = \frac{p^2}{2m} + V_{ECP} + \frac{\mu_B}{\hbar}(\boldsymbol{L} + g_S\boldsymbol{S} + g_I\boldsymbol{I})\boldsymbol{B}(t) + \eta\boldsymbol{LS} + A_{hfs}\boldsymbol{IJ} \quad , \tag{1.1}$$

in which we recognize four different terms:

1. **Coulomb Interaction**: the first two terms are the Kinetic one, with m the mass of the electron, and the Coulomb interaction, represented by the effective core potential composed of the effective core charge divided by the distance from the nucleus: $V_{ECP} = -\frac{Z_{eff}}{r}$.

2. **Zeeman Coupling**: the third term is given by the interaction between the angular degree of freedom with the external magentic field $\mathbf{B}(t)$. In particular there are the angular momentum and the spin of the electron, $\mathbf{L}$ and $\mathbf{S}$, and the nuclear spin $\mathbf{I}$. In this term μ_B is the Bohr magneton while g_S and g_I are the Landé g-factors.

3. **Spin-Orbit Interaction**: the fourth term is given by the interaction between the angular momentum and the spin of the electron. In it appears $\eta = \frac{Z^4\alpha^2}{n^3}$, where α is the fine structure constant and n is the principal quantum number.

4. **Hyperfine Interaction**: the last term is the interaction between the total angular momentum of the electron $\mathbf{J} = \mathbf{L} + \mathbf{S}$ with the nuclear spin. A_{hfs} is the hyperfine-structure constant which is determined by experiment.

1.1.1 Breit-Rabi Formula

As it will be used as a test to validate the new implementation of RT-TDHF, a simple explanation of the Breit-Rabi formula is given (for a detailed derivation see [3]).
Focusing on the Zeeman and hyperfine interaction of the Hamiltonian in Eq.1.1, is possible to find an approximate solution of the spectrum in two different regime. In situations where magnetic fields are weak, the Zeeman interaction is treated as a perturbation to the basis states given by the quantum number $\boldsymbol{F} = \boldsymbol{I} + \boldsymbol{J}$ and its projections m_F. However, when the magnetic field is strong, the Zeeman effect becomes dominant, and becomes necessary to change the quantum number used to describe the states to $|\boldsymbol{I}, \boldsymbol{J}, m_I, m_J\rangle$. Nevertheless, since we are interested in a wide range of magnetic field strengths, eigenstates that are a superposition of the $|\boldsymbol{F}, m_F\rangle$ and $|\boldsymbol{I}, \boldsymbol{J}, m_I, m_J\rangle$ basis states must be considered. In the particular case in which the orbital angular momentum is zero, such as in $^9Be^+$, it is possible to solve the Hamiltonian analytically. The spectrum is then given by the Breit-Rabi formula:

$$\Delta E_{F=I\pm\frac{1}{2}} = -\frac{h\Delta W}{2(2I+1)} + \mu_B g_I m_F B \pm \frac{h\Delta W}{2}\sqrt{1 + \frac{2m_F x}{I+\frac{1}{2}} + x^2} \quad , \tag{1.2}$$

$$x \equiv \frac{B(\mu_\mathrm{B} g_J - \mu_\mathrm{B} g_I)}{h\Delta W} \quad \Delta W = A\left(I + \frac{1}{2}\right) \quad , \tag{1.3}$$

with

$$g_J = \frac{J(J+1) + L(L+1) - S(S+1)}{2J(J+1)} + g_S\frac{J(J+1) - L(L+1) + S(S+1)}{2J(J+1)} \quad . \tag{1.4}$$

Although the energies in Eq.1.2 are indexed by the quantum numbers F and m_F, it is crucial to note that these are not good quantum numbers. This implies that the relative eigenstates do not possess definite F and m_F, but rather are superpositions of states with definite F and m_F.

1.2 External State

The degree of freedom relative to the motion of the ion goes under the name of external state. In the context of ion traps, the motion is governed in an approximated way by an harmonic potential. In R. Husistein's work [2] the external state was simulated using Hagedorn wave packets in order to adapt the description also to non-harmonic potentials as well.

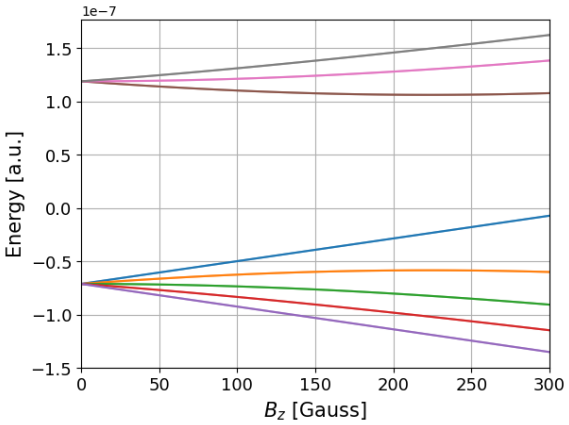

Figure 1.1: Breit-Rabi diagram, showing the splitting in energy as a function of an external magnetic field.

1.3 Full System

To accurately simulate the entire system, it is necessary to establish a connection between the internal state and the external state of the ion. Moreover, it's crucial to demonstrate that these states are entangled, indicating a coupling between the internal state and the position of the ion. R. Husistein demonstrated that a reliable method to verify the accurate implementation, and thus the entanglement between the two states, is to observe the "collapse and revival" phenomenon as described by the James-Cummings model [4].

1.4 Extended RT-TDHF

As previously outlined, the objective of this project is to expand upon R. Husistein's work on internal states by incorporating the hyperfine interaction and a time-varying magnetic field. This implies adapting the RT-TDHF method to a Hamiltonian that includes a time-dependent magnetic field, as described in Eq. 1.1. The upcoming section will provide a brief overview of the Hartree-Fock method for a spin-less system (for a more detailed derivation see [5]), followed by the formalism and derivation required to extend the Roothaan equation Eq.1.13 to a wavefunction incorporating both electron spin and nuclear spin.

1.5 Hartree-Fock Method

Let us start taking in account the simplest Hamiltonian governing the motion of electrons in an atom in atomic units, composed of the kinetic term of the electrons, the interaction between the electrons and the nucleus and the pairwise interactions between all electrons:

$$H = \sum_i (-\frac{1}{2}\nabla_i^2 - \frac{Z}{|\boldsymbol{r}_i - \boldsymbol{R}|}) + \frac{1}{2}\sum_{i,j}\frac{1}{|\boldsymbol{r}_i - \boldsymbol{r}_j|} \quad , \tag{1.5}$$

in which the sums run over all the electrons, $\mathbf{R}$ is the position of the nucleus, and Z is the total charge of the nucleus. To simplify the notation we can define the single electron Hamiltonian h_i and the two electron operator $g_{i,j}$ as follows :

$$h_i = -\frac{1}{2}\nabla_i^2 - \frac{Z}{|\boldsymbol{r}_i - \boldsymbol{R}|} \quad , \tag{1.6}$$

$$g_{i,j} = \frac{1}{|\boldsymbol{r}_i - \boldsymbol{r}_j|} \quad . \tag{1.7}$$

It is possible to express a generic anti-symmetric wavefunction, denoted as $\Psi(\mathbf{r}_1, \ldots, \mathbf{r}_N)$, as a single Slater determinant formed from single-particle orbital wavefunctions $\psi_k(\mathbf{r}_i)$, where k represents some quantum number associated with the particle.
It's crucial to recognize that while the Hartree-Fock method represents the total wavefunction as a single Slater determinant, it inherently fails to fully account for correlation effects arising from the interactions within the multi-electron system. However, for our specific case of interest, the $^9Be^+$ ion, which contains only one electron in the valence shell, correlation effects are relatively insignificant and can be safely disregarded. By neglecting correlation effects, we simplify our computational approach, making the Hartree-Fock method a suitable and efficient tool for describing the electronic structure of the $^9Be^+$ ion.
In the Hartree-Fock method, the variational principle plays a central role in determining the optimal set of orbitals. This principle states that for any trial wavefunction $|\psi\rangle$, the expectation value of the Hamiltonian is always greater than or equal to the true ground-state energy of the system:

$$\langle\psi| H |\psi\rangle \geq E_0 \tag{1.8}$$

By varying the orbitals within the Slater determinant, the Hartree-Fock method seeks to minimize the energy expectation value, effectively finding the best approximation to the true ground-state wavefunction within the chosen basis set.

Minimizing Eq.1.8 with the constraint that all the orbitals must be orthonormal and defining the Coulomb and Exchange operators as:

$$J\psi(\boldsymbol{r}) = \sum_k \int d^3r' \frac{|\psi_k(\boldsymbol{r'})|^2}{|\boldsymbol{r} - \boldsymbol{r'}|}\psi(\boldsymbol{r}) \quad , \tag{1.9}$$

$$K\psi(\boldsymbol{r}) = \sum_k \int d^3r' \frac{\psi_k^*(\boldsymbol{r'})\psi(\boldsymbol{r'})}{|\boldsymbol{r} - \boldsymbol{r'}|}\psi_k(\boldsymbol{r}) \quad , \tag{1.10}$$

it is possible to derive the following eigenvalue equation for the so called Fock operator:

$$\mathcal{F}|\psi_k\rangle := (h + J - K)|\psi_k\rangle = \epsilon_k |\psi_k\rangle \quad . \tag{1.11}$$

To enable efficient and analytical computation of the necessary integrals in the Hartree-Fock method, a common strategy involves expanding each orbital using a finite set of Gaussian-type orbitals (GTOs). By representing the molecular orbitals as linear combinations of GTOs, it is possible approximate their shapes and behaviors with high accuracy while simplifying the integration process:

$$|\psi_k\rangle = \sum_\mu C_{k,\mu} |\chi_\mu\rangle \quad . \tag{1.12}$$

Keeping in mind that these new orbitals might be not orthogonal in general, we can rewrite Eq.1.11 in to the Roothaan equation:

$$F\boldsymbol{C}_k = \epsilon_k S\boldsymbol{C}_k \quad , \tag{1.13}$$

in which we defined the Fock operator in the new basis as: $F_{\mu\nu} = \langle\chi_\mu|\mathcal{F}|\chi_\nu\rangle$, the overlap matrix as: $S_{\mu\nu} = \langle\chi_\mu|\chi_\nu\rangle$, and the coefficient vector $\boldsymbol{C}_k = (C_{k,1}, ..., C_{k,\mu}, ...)^T$.

1.6 Electron Spin

Since we want to extend the Hamiltonian to take into account also an external magnetic field, we need to modify the method developed so far to introduce the spin of the electron. In order to do so, we can simply rewrite the single particle functions as a superposition of spin-up and spin-down states:

$$\psi_k(\boldsymbol{r}) := \begin{pmatrix} \phi_k^+(\boldsymbol{r}) \\ \phi_k^-(\boldsymbol{r}) \end{pmatrix} = \sum_\mu C_{\mu k}^+ \chi_\mu(\boldsymbol{r}) \left|+\right\rangle + \sum_\mu C_{\mu k}^- \chi_\mu(\boldsymbol{r}) \left|-\right\rangle \quad , \tag{1.14}$$

in which we defined the spin-up orbital $\phi_k^+(\mathbf{r})$ and the spin-down orbital $\phi_k^-(\mathbf{r})$ as a superposition of GTOs.
Thus, we can rewrite Eq. 1.13 in matrix form:

$$\begin{pmatrix} F^{++} & F^{+-} \\ F^{-+} & F^{--} \end{pmatrix} \begin{pmatrix} \boldsymbol{C}_k^+ \\ \boldsymbol{C}_k^- \end{pmatrix} = \epsilon_k \begin{pmatrix} S\boldsymbol{C}_k^+ \\ S\boldsymbol{C}_k^- \end{pmatrix} \quad . \tag{1.15}$$

Next, we just need to understand the shape of each block of the Fock operator:

$$F_{\mu\nu}^{\alpha\beta} = \left\langle \chi_\mu, \alpha \right| \mathcal{F} \left| \chi_\nu, \beta \right\rangle = \left\langle \chi_\mu, \alpha \right| h + J - K \left| \chi_\nu, \beta \right\rangle \quad , \tag{1.16}$$

in which we used the notation $\langle \mathbf{r} | \chi_\mu, \alpha \rangle = \chi_\mu(\mathbf{r}) \left|\alpha\right\rangle$, with α and β equal to + or -.

We will look at the precise shape of h when we will extend the one electron Hamiltonian, and for now we can simply write: $\left\langle \chi_\mu, \alpha \right| h \left| \chi_\nu, \beta \right\rangle = h_{\mu\nu}^{\alpha\beta}$. Our immediate focus is on defining the explicit expressions for the Coulomb and exchange operators:

- **Coulomb Operator**: Since the Coulomb operator is spin independent, is diagonal in the GTOs basis. Nevetheless, each spin block of the coulomb operator contributes to the final result (see [6]):

$$\begin{aligned} \left\langle \mu, \alpha \right| J \left| \nu, \beta \right\rangle =& \delta_{\alpha\beta} \sum_k \int d^3 r_1 d^3 r_2 \frac{\chi_\mu^*(\boldsymbol{r_1}) \chi_\nu(\boldsymbol{r_1})}{|\boldsymbol{r_1} - \boldsymbol{r_2}|} (|\phi_k^+(\boldsymbol{r_2})|^2 + |\phi_k^-(\boldsymbol{r_2})|^2) = \\ :=& \delta_{\alpha\beta}(J_{\mu\nu}^{++} + J_{\mu\nu}^{--}) \quad . \end{aligned} \tag{1.17}$$

  By defining the density operator as:

$$P_{\mu\nu}^{\alpha\beta} = \sum_k C_{\mu k}^\alpha C_{\nu k}^{\beta *} \quad , \tag{1.18}$$

  it is possible to rewrite each term of the Coulomb operator in the following way:

$$J_{\mu\nu}^{\alpha\alpha} = \sum_{\sigma\rho} P_{\sigma\rho}^{\alpha\alpha} \left\langle \chi_\mu, \chi_\rho \right| g \left| \chi_\nu, \chi_\sigma \right\rangle \quad . \tag{1.19}$$

- **Exchange Operator**: Even if also the exchange operator is not spin dependent, this won't be diagonal. This is due to the fact that it changes the quantum numbers (such as spin) of the function over which it is applied with the one it integrates, as is possible to verify in Eq.1.10. Also in this case we can rewrite the operator as a function of the density operator:

$$K_{\mu\nu}^{\alpha\beta} = \left\langle \mu, \alpha \right| J \left| \nu, \beta \right\rangle = \sum_{\sigma\rho} P_{\sigma\rho}^{\alpha\alpha} \left\langle \chi_\mu, \chi_\rho \right| g \left| \chi_\sigma, \chi_\nu \right\rangle \quad . \tag{1.20}$$

In the end we can write a generic block of the Fock matrix defined in Eq.1.15 as:

$$F^{\alpha\beta} = h^{\alpha\beta} + \delta^{\alpha\beta}(J^{++} + J^{--}) - K^{\alpha\beta} \quad . \tag{1.21}$$

1.7 Nuclear Spin

The next step which is needed to be taken is to introduce another degree of freedom to the wavefunction: the spin of the nucleus. This will be crucial in order to introduce the hyper-fine interaction in our model for the atom. Following a similar approach as with electron spin, firstly it is needed to increase the dimensionality of the wavefunction. Assuming that the nucleus has spin equal to **I**, it is possible to represent the wavefunction as a superposition over each spin projections:

$$\psi_k(\boldsymbol{x}) \otimes |I\rangle = \sum_{\mu} \sum_{i=-I}^{I} (C_{\mu k}^{+,i} |\mu, +, i\rangle + C_{\mu k}^{-,i} |\mu, -, i\rangle) \quad , \tag{1.22}$$

in which we added the nuclear spin degree of freedom m_I with $|i\rangle$ and used the notation $|\chi_\mu\rangle = |\mu\rangle$ for simplicity.
Again, the dimension of the Fock matrix in Eq.1.15 has to further extended to $2(2I+1) \times 2(2I+1)$:

$$\begin{pmatrix} \hat{F}_{I,I} & \hat{F}_{I,I-1} & \dots & \hat{F}_{I,-I} \\ \hat{F}_{I-1,I} & \ddots & & \vdots \\ \vdots & & \ddots & \\ \hat{F}_{-I,I} & \dots & & \hat{F}_{-I,-I} \end{pmatrix} \begin{pmatrix} \hat{C}_k^I \\ \hat{C}_k^{I-1} \\ \vdots \\ \hat{C}_k^{-I} \end{pmatrix} = \epsilon_k \begin{pmatrix} S\hat{C}_k^I \\ S\hat{C}_k^{I-1} \\ \vdots \\ S\hat{C}_k^{-I} \end{pmatrix} , \tag{1.23}$$

in which:

$$\hat{C}_k^i = \begin{pmatrix} \boldsymbol{C}_k^{+,i} \\ \boldsymbol{C}_k^{-,i} \end{pmatrix} \quad , \qquad \hat{F}_{i,j} = \begin{pmatrix} \hat{F}_{i,j}^{++} & \hat{F}_{i,j}^{+-} \\ \hat{F}_{i,j}^{-+} & \hat{F}_{i,j}^{--} \end{pmatrix} \quad . \tag{1.24}$$

The results derived for the electron spin in the previous section can be used to write each block of the Fock matrix. In order to do so the definition of the density matrix must be changed in the following way:

$$(P_{i,j}^{\alpha\beta})_{\mu\nu} = \sum_k C_{\mu k}^{\alpha i} (C_{\nu k}^{\beta j})^* \quad . \tag{1.25}$$

As before, the Coulomb operator is not spin dependent also in the case of the nuclear spin, and therefore it is sufficient to simply redefine each element of it:

$$(J_{ii}^{\alpha\alpha})_{\mu\nu} = \sum_{\sigma\rho} (P_{i,i}^{\alpha\alpha})_{\mu\nu} \langle \chi_\mu, \chi_\rho | \, g \, | \chi_\nu, \chi_\sigma \rangle \quad . \tag{1.26}$$

As before the exchange operator is not diagonal and but each element can be simply written as follow:

$$(K_{ij}^{\alpha\beta})_{\mu\nu} = \sum_{\sigma\rho} (P_{i,j}^{\alpha\beta})_{\mu\nu} \langle \chi_\mu, \chi_\rho | \, g \, | \chi_\sigma, \chi_\nu \rangle \quad . \tag{1.27}$$

In the end a generic element of the Fock matrix can be written as:

$$F_{ij}^{\alpha\beta} = h_{ij}^{\alpha\beta} + \delta_{ij}\delta^{\alpha\beta} \sum_{l=-I}^{+I} (J_{ll}^{++} + J_{ll}^{--}) - K_{ij}^{\alpha\beta} \quad . \tag{1.28}$$

1.8 Generalize the Hamiltonian

With the Coulomb and exchange operators now adapted to include both nuclear and electronic spin, our remaining task is to extend the Hamiltonian to incorporate

interaction with a time-varying external field. These additional terms will manifest in the one-electron term h of the Fock matrix. Consequently, we can express the interaction for a single electron as:

$$h = \frac{p^2}{2m} - \frac{Z}{|\boldsymbol{r}-\boldsymbol{R}|} + \frac{\mu_B}{\hbar}(\boldsymbol{L} + g_S\boldsymbol{S} + g_I\boldsymbol{I})\boldsymbol{B}(t) + \eta\boldsymbol{L}\boldsymbol{S} + A_{hfs}\boldsymbol{I}\boldsymbol{J} \quad . \tag{1.29}$$

Before analysing each term, we recall the following identities for the electron spin:

$$S_x\left|\pm\right\rangle = \frac{\hbar}{2}\left|\mp\right\rangle \quad , \quad S_y\left|\pm\right\rangle = \pm\frac{\hbar}{2}i\left|\mp\right\rangle \quad , \quad S_z\left|\pm\right\rangle = \pm\frac{\hbar}{2}\left|\pm\right\rangle \quad , \tag{1.30}$$

and for the nuclear spin:

$$\begin{aligned}
\langle i|\, I_x\,|j\rangle &= \frac{\hbar}{2}\Big(\delta_{ij+1}\sqrt{I(I+1)-j(j+1)} + \delta_{ij-1}\sqrt{I(I+1)-j(j-1)}\Big) \quad , \\
\langle i|\, I_y\,|j\rangle &= \frac{i\hbar}{2}\Big(-\delta_{ij+1}\sqrt{I(I+1)-j(j+1)} + \delta_{ij-1}\sqrt{I(I+1)-j(j-1)}\Big) \quad , \\
\langle i|\, I_z\,|j\rangle &= \delta_{ij}\hbar j \quad .
\end{aligned} \tag{1.31}$$

Now we can start rewriting each term of $(h_{ij}^{\alpha\beta})_{\mu\nu}$:

1. The first two terms are diagonal in the spin-block representation:

$$\langle\mu,\alpha,i|\, h_0\,|\nu,\beta,j\rangle = \langle\mu,\alpha,i|\, \frac{p^2}{2m} - \frac{Z}{|\boldsymbol{r}-\boldsymbol{R}|}\,|\nu,\beta,j\rangle = \delta^{\alpha\beta}\delta_{ij}\,\langle\mu|\, h_0\,|\nu\rangle \quad , \tag{1.32}$$

   therefore each block can be written as:

$$\hat{h}_0^{ii} = \langle\mu|\, h_0\,|\nu\rangle \otimes 1_{2\times 2} \quad . \tag{1.33}$$

2. Also the coupling between the angular momentum and the external field is diagonal:

$$\langle\mu,\alpha,i|\, h_{BL}\,|\nu,\beta,j\rangle = \langle\mu,\alpha,i|\, \frac{\mu_B}{\hbar}\boldsymbol{L}\boldsymbol{B}(t)\,|\nu,\beta,j\rangle = \delta^{\alpha\beta}\delta_{ij}\,\langle\mu|\, h_{BL}\,|\nu\rangle \quad , \tag{1.34}$$

   which leads to:

$$\hat{h}_{BL}^{ii} = \frac{\mu_B}{\hbar}\boldsymbol{B}(t)\,\langle\mu|\,\boldsymbol{L}\,|\nu\rangle \otimes 1_{2\times 2} \quad . \tag{1.35}$$

3. The Zeeman term can be written in a block-diagonal form by using Eq.1.30:

$$\begin{aligned}
\langle\mu,\alpha,i|\, h_{BS}\,|\nu,\beta,j\rangle &= \langle\mu,\alpha,i|\, \frac{\mu_B g_S}{\hbar}\boldsymbol{S}\boldsymbol{B}(t)\,|\nu,\beta,j\rangle = \delta_{ij}\frac{\mu_B g_S}{\hbar}\boldsymbol{B}(t)S_{\mu\nu}\,\langle\alpha|\,\boldsymbol{S}\,|\beta\rangle \\
\Rightarrow \hat{h}_{BS}^{ii} &= \frac{\mu_B g_S}{2}\begin{pmatrix} B_z(t)S & (B_x(t)-iB_y(t))S \\ (B_x(t)+iB_y(t))S & -B_z(t)S \end{pmatrix} \quad .
\end{aligned} \tag{1.36}$$

4. In the same way we can rewrite the spin orbit coupling, which is also block diagonal:

$$\hat{h}_{LS}^{ii} = \frac{\eta}{2}\begin{pmatrix} L_z & L_x - iL_y \\ L_x + iL_y & -L_z \end{pmatrix} \quad . \tag{1.37}$$

5. The interaction between the nuclear spin and the external field produces diagonal blocks in all the Fock matrix:

$$\langle\mu,\alpha,i|\, h_{BI}\,|\nu,\beta,j\rangle = \langle\mu,\alpha,i|\, \frac{\mu_B g_I}{\hbar}\boldsymbol{I}\boldsymbol{B}(t)\,|\nu,\beta,j\rangle = \delta^{\alpha\beta}\frac{\mu_B g_I}{\hbar}S_{\mu\nu}\boldsymbol{B}(t)\,\langle i|\,\boldsymbol{I}\,|j\rangle \quad , \tag{1.38}$$

   from which we have:

$$\hat{h}_{BI}^{ij} = \frac{\mu_B g_I}{\hbar}\boldsymbol{B}(t)(S\,\langle i|\,\boldsymbol{I}\,|j\rangle) \otimes 1_{2\times 2} \quad . \tag{1.39}$$

6. The last term, the interaction between the total electronic momentum and the nuclear spin, can be split in two terms. The first produces diagonal blocks:

$$\langle \mu, \alpha, i | \, h_{IL} \, | \nu, \beta, j \rangle = \langle \mu, \alpha, i | \, A_{hfs} \boldsymbol{IL} \, | \nu, \beta, j \rangle \quad , \tag{1.40}$$

from which we have:

$$\hat{h}_{IL}^{ij} = A_{hfs} (\langle i | \, \boldsymbol{I} \, | j \rangle \, \langle \mu | \, \boldsymbol{L} \, | \nu \rangle) \otimes 1_{2\times 2} \quad . \tag{1.41}$$

On the other hand the last one is not diagonal, nor block diagonal:

$$\langle \mu, \alpha, i | \, h_{IS} \, | \nu, \beta, j \rangle = \langle \mu, \alpha, i | \, A_{hfs} \boldsymbol{IS} \, | \nu, \beta, j \rangle \quad , \tag{1.42}$$

which we can rewrite as:

$$\hat{h}_{IS}^{ij} = \frac{A_{hfs}}{2} \begin{pmatrix} \delta_{ij} \hbar j S & (\langle i | \, I_x \, | j \rangle - i \, \langle i | \, I_y \, | j \rangle) S \\ (\langle i | \, I_x \, | j \rangle + i \, \langle i | \, I_y \, | j \rangle) S & -\delta_{ij} \hbar j S \end{pmatrix} \quad . \tag{1.43}$$

Ultimately, we may incorporate into the Hamiltonian, as expressed in Eq.1.29, the interaction between the ion and an external time-varying electric field. Notably, this interaction excludes the two degrees of freedom related to the nuclear and electronic spin, resulting in the generation of only diagonal terms in the block representation. Subsequently, employing the dipole approximation allows us to represent the new interaction in the Fock matrix as follows:

$$\hat{h}_{d}^{ii} = \boldsymbol{E}(t) \cdot \langle \mu | \, \boldsymbol{r} \, | \nu \rangle \otimes 1_{2\times 2} \quad . \tag{1.44}$$

With all the expressions for the individual blocks of the Hamiltonian at hand, one can easily construct the full one electron part of the Fock operator, and evaluate the energy of the system with (see [7]):

$$E = \frac{1}{2} Tr[P(h + F)] \quad , \tag{1.45}$$

in which h represents the full one electron part of the Fock operator.

1.9 Time Evolution

Having at hand the density and the full Fock operator as expressed in Eq.1.28, a suitable time integration scheme has to be chosen in order to numerically solve the Liouville-von Neumann equation, as explained in [8]:

$$\frac{dP(t)}{dt} = [F(t), P(t)] \quad . \tag{1.46}$$

One needs to recall that the above equation is valid only if the matrix are written in an orthogonal basis. Therefore, the first step that has to be taken is to use the Lowdin orthogonalization method, as explained in [9]:

$$P = S'^{1/2} P' (S'^{1/2})^T, \quad F = (S'^{-1/2})^T F' S'^{-1/2} \quad . \tag{1.47}$$

As time integration scheme we will adopt the same method used by R. Husistein in [2], the explicit second-order (trapezoidal) Magnus propagator:

$$\begin{aligned} U_{FE}(t_k) &= \exp(-i \Delta t F(P(t_k), t_k)), \\ P_{FE}(t_{k+1}) &= U_{FE}(t_k) P(t_k) U_{FE}^{\dagger}(t_k), \\ F_m(t_k, t_{k+1}) &= \frac{1}{2}(F(P(t_k), t_k) + F(P_{FE}(t_{k+1}), t_{k+1})), \\ U_{EM2}(t_k) &= \exp(-i \Delta t F_m(t_k, t_{k+1})), \\ P(t_{k+1}) &= U_{EM2}(t_k) P(t_k) U_{EM2}^{\dagger}(t_k). \end{aligned}$$

Chapter 2

Results

The extended implementation of RT-TDHF algorithm was tested in order to validate its accuracy and reliability. The tests were conducted focusing on simulating the behavior of the $^9Be^+$ ion. To effectively model the electronic structure of this ion, BFD-PP pseudopotential [10] was employed as the chosen effective core potential. The selection of the BFD-PP aimed at achieving a closer approximation of the ion's behavior within the computational framework.
The computational simulation of the $^9Be^+$ ion also employed the cc-pVDZ basis set. The cc-pVDZ (Correlation-consistent Polarized Valence Double Zeta) basis set [11] is widely recognized for its accuracy in describing molecular electronic structure while offering computational efficiency.
Given the choice of the ECP and of the basis set it was possible to use the pySCF package [12] to efficiently compute the required integrals for the method (angular momentum, overlap, nuclear potential, kinetic, dipole, Coulomb and exchange integrals). In addition to this, the basic Hartee-Fock method already implemented in pySCF, for the simple Hamiltonian given in eq.1.5, was used to achieve a first guess of the density matrix.
In conclusion, the coefficients used in the Hamiltonian in Eq.1.29 are reported in Tab.2.1.

Constant	Value
μ_b [J/T]	$9.27400968 \cdot 10^{-24}$
g_S	2.0023193043622
g_I	$g_S \cdot 2.134779853 \cdot 10^{-4}$
A_{hfs} [MHz]	-625.008837048

Table 2.1: Physical Constants for $^9Be^+$ ion.

2.1 Hyperfine Splitting

By computing the average energy of the states $|F, m_F\rangle$, where $\boldsymbol{F} = \boldsymbol{I} + \boldsymbol{J} = \boldsymbol{I} + \boldsymbol{S}$, under zero external field conditions, we derived the hyperfine caused by $A_{hfs}\boldsymbol{I} \cdot \boldsymbol{J}$. As our method operates with a density matrix formulated in the $|m_I, m_S\rangle$ basis, it necessitated an initial transformation of the $|F, m_F\rangle$ states into this appropriate basis. This transformation was accomplished using Clebsch-Gordan coefficients.
The energies obtained with the simulation are compared to their theoretical value given by Eq.1.2, and are reported in Tab.2.2. The energies obtained with the

simulation are in agreement with their theoretical values, showing the correct implementation of the hyperfine term in the new Hamiltonian.

State	Energy [GHz]	Theo. Energy [GHz]	Relative Error
$\|2,2\rangle$	$-4.6875663 \cdot 10^{-1}$	$-4.6875656 \cdot 10^{-1}$	$1.467 \cdot 10^{-7}$
$\|2,1\rangle$	$-4.6875663 \cdot 10^{-1}$	$-4.6875656 \cdot 10^{-1}$	$1.405 \cdot 10^{-7}$
$\|2,0\rangle$	$-4.6875663 \cdot 10^{-1}$	$-4.6875656 \cdot 10^{-1}$	$1.483 \cdot 10^{-7}$
$\|2,-1\rangle$	$-4.6875663 \cdot 10^{-1}$	$-4.6875656 \cdot 10^{-1}$	$1.421 \cdot 10^{-7}$
$\|2,-2\rangle$	$-4.6875663 \cdot 10^{-1}$	$-4.6875656 \cdot 10^{-1}$	$1.467 \cdot 10^{-7}$
$\|1,1\rangle$	$7.8126105 \cdot 10^{-1}$	$7.8126093 \cdot 10^{-1}$	$1.458 \cdot 10^{-7}$
$\|1,0\rangle$	$7.8126104 \cdot 10^{-1}$	$7.8126093 \cdot 10^{-1}$	$1.421 \cdot 10^{-7}$
$\|1,-1\rangle$	$7.8126105 \cdot 10^{-1}$	$7.8126093 \cdot 10^{-1}$	$1.449 \cdot 10^{-7}$

Table 2.2: Energy obtained with the simulation and with the exact formula Eq.1.2. The Relative error is evaluated as $\frac{|E-E_{theo}|}{|E_{theo.}|}$.

2.2 Breit-Rabi Diagram

In our exploration of the magnetic field-dependent part of the Hamiltonian, we aimed to replicate the Breit-Rabi diagram. As delineated in the theoretical section, gradually transitioning from weak to strong magnetic field causes shifts in the eigenstates of the Hamiltonian. Consequently, to accurately achieve the mean energy for the diagram, we needed to adapt the set of simulated states and, correspondingly, the density matrices for each magnetic field strength. Achieving this necessitated the exact diagonalization of the Hamiltonian, comprising both the hyperfine term and the magnetic interaction, expressed in the basis $|m_I, m_S\rangle$. Thus, in each iteration, we employed the exact eigenvectors of the Hamiltonian to construct the required density matrices. The energies were computed across a spectrum of 100 magnetic field strengths ranging from 0 to 300 Gauss. The results are shown in Fig.2.1. Also in this case the results confirm the validity of the new implementation.

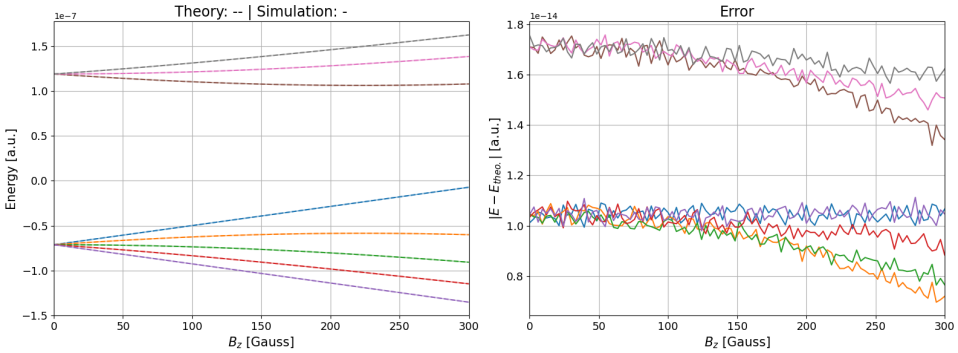

Figure 2.1: Comparison between the exact Breit-Rabi diagram obtained with Eq.1.2 and the simulation.

2.3 Time Comparison

Ultimately, two time evolution simulations were conducted: one for the hydrogen atom and the other for the $^9Be^+$ ion, over a period of $T = 10$ a.u. with varying time

steps dt. An external magnetic field along the z-axis of $B_z = 100$Gauss was applied during all the time evolution. Each simulation has been repeated 10 times.
The simulations utilized both the newest implementation, which accounts for nuclear spin and the new terms in the Hamiltonian, and the previous internal state implementation as shown in [2].
These tests were performed to compare the runtime differences between the two algorithms.

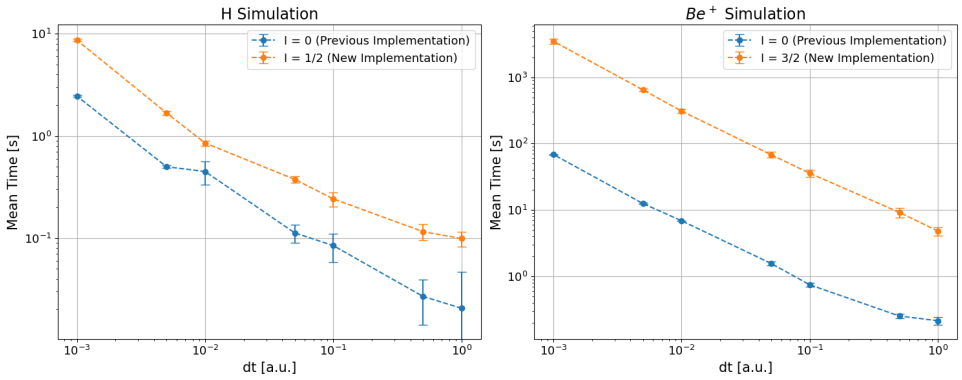

Figure 2.2: Runtime comparison between the previous implementation [2] (without nuclear spin, Zeeman and hyperfine interaction) and the new one. The simulations were conducted over a period of $T = 20$ a.u., with an external magnetic field directed along the z-axis of $B_z = 100$ Gauss.

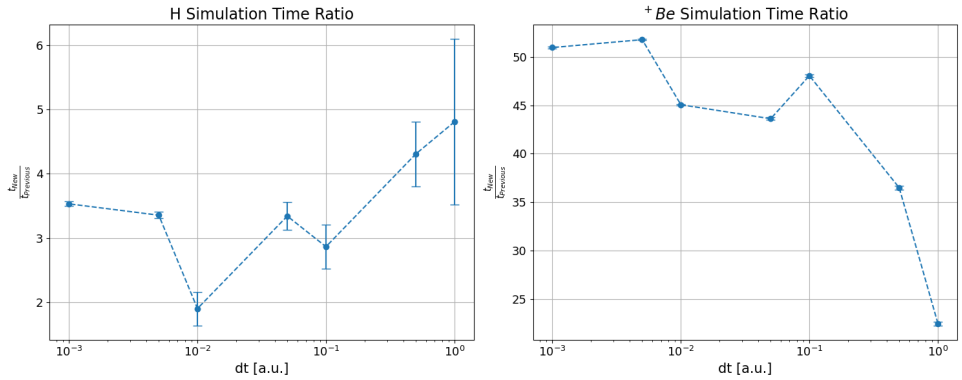

Figure 2.3: Ratio between the runtime of the new implementation and the previous one [2].

As illustrated in Fig.2.2 and 2.3, the new implementation requires more time. This increased computational demand is due to the incorporation of the new spin degree of freedom, which necessitates the use of larger matrices in the simulation. Consequently, as the nuclear spin increases, so does the computational cost.

Conclusions

In this work, the Real-Time Time-Dependent Hartree-Fock (RT-TDHF) algorithm was extended to include the effects of nuclear spin. In order to do so, the hyperfine interactions and the Zeeman coupling between the spin degree of freedom and a time varying magnetic field were taken into account. The simulations were focused on the $^9Be^+$ ion, utilizing the Berkeley-Cranium-Bonner-Feinberg Pseudopotential (BFD-PP) and the cc-pVDZ basis set to achieve a approximation of the ground state energy of the system.
The required equations for the new algorithm were derived starting from the Hartree-Fock method, modifying the exchange and Coulomb integrals and the core one electron Hamiltonian of the system.

The accuracy of the implementation was then validated by computing the hyperfine splitting and comparing the simulated energy levels to theoretical values. The results, reported in Tab.2.2 , demonstrated an excellent agreement between the simulation and theoretical predictions, confirming the correct inclusion of the hyperfine term in the Hamiltonian.
Additionally, the behavior of the ion under varying magnetic field strengths was investigated by replicating the Breit-Rabi diagram. The results, shown in Fig.2.1 , further confirmed the validity of the new implementation, accurately capturing the shifts in eigenvalues due to magnetic interactions.
A time comparison between the new implementation and the previous version developed in [2], which did not account for nuclear spin and hyperfine interactions, revealed an expected increase in computational demand. This increase, shown in Fig.2.2 and Fig.2.3, is attributed to the inclusion of the new nuclear spin degree of freedom, necessitating the use of larger matrices in the simulation.
In conclusion, the extended RT-TDHF algorithm proves to be a robust and accurate method for simulating systems having hyperfine interactions and in the presence of a time varying electromagnetic field.

In order to simulate the full system composed of the internal and external states, further work needs to be done. First of all, the new implementation should be combined with the external state simulation shown in [2], and the collapse and revival phenomena should be observed to ensure the entanglement between the two states.
As an alternative, the RT-TDHF method could be further extended to the real-time time-dependent nuclear-electronic orbital Hartree-Fock (RT-NEO-TDHF) method [13]. This approach would allow for the simultaneous simulation of both internal and external states without relying on the Born-Oppenheimer approximation. Consequently, after proper implementation, it would eliminate the need to combine the two states and check for the proper entanglement.
Additionally, the algorithm should be further extended to take in account more than one ion, in order to fully simulate a storage ring. For the internal state, the extended RT-TDHF method can be employed with minor modifications to account for the increased number of ions. However, it is important to note that this method

introduces an inherent error because the HF method, due to its single determinant approximation, does not account for correlation effects.
Ultimately, accounting for the presence of multiple ions and properly addressing the entanglement between the internal and external states should be sufficient to simulate the entire storage ring and study its decoherence time.

Appendix

A.1 Source Code

The complete code developed during this project is available at `https://gitlab.ethz.ch/heinekas/quantumbeam/-/tree/solinas_m_semester_thesis/husistein_r_master_project/internal_state_energy/rt-tdhf?ref_type=heads`. The implementation of the extended RT-TDHF can be found in "rttdhf_simulation_copy.py" and all the tests done in the jupyter notebook "Test.ipynb". In particular:

- Tab.2.2 can be reproduced with "Test.ipynb" in the section "Rabi Formula/Hyperfine Energy".
- Fig.2.1 can be reproduced with "Test.ipynb" in the section "Rabi Formula/Simulation changing eigenvectors".
- Fig.2.2 and Fig.2.3 can be reproduced with "Test.ipynb" in the section "Time Comparison".
- A simple example that shows how to properly call the class and perform a time propagation can be found in "Test.ipynb" under the section "General Test for the class".

References

[1] K. A. Brown and T. Roser, "Towards storage rings as quantum computers," *Phys. Rev. Accel. Beams*, vol. 23, p. 054 701, 5 May 2020. DOI: 10.1103/PhysRevAccelBeams.23.054701. [Online]. Available: https://link.aps.org/doi/10.1103/PhysRevAccelBeams.23.054701.

[2] R. T. Husistein. "Simulation of phonon states in accelerators." Version: 2023. (2023), [Online]. Available: https://gitlab.psi.ch/AMAS-students/Husistein_R/-/blob/737802573465f41cca1aa8b7f5707193266bea2e/master_project/report/thesis.pdf.

[3] G. K. Woodgate, *Elementary atomic structure*. Oxford: Clarendon Press, 1980.

[4] C. Hempel, *Digital quantum simulation, schrödinger cat state spectroscopy and setting up a linear ion trap*, Available from INIS: http://inis.iaea.org/search/search.aspx?orig_q=RN:47078884; Available from INIS in electronic form. Also available from Library of the University of Innsbruck, Innrain 50, 6020 Innsbruck (AT) and available from http://permalink.obvsg.at/AC11359136, 2014.

[5] J. Thijssen, "The hartree–fock method," in *Computational Physics*. Cambridge University Press, 2007, pp. 43–88.

[6] F. Ding, J. Goings, M. Frisch, and X. Li, "Ab initio non-relativistic spin dynamics," *The Journal of chemical physics*, vol. 141, p. 214 111, Dec. 2014. DOI: 10.1063/1.4902884.

[7] A. Szabo and N. S. Ostlund, *Modern Quantum Chemistry: Introduction to Advanced Electronic Structure Theory*. Dover Publications Inc., 1996.

[8] X. Li, S. M. Smith, A. N. Markevitch, D. A. Romanov, R. J. Levis, and H. B. Schlegel, "A time-dependent hartree–fock approach for studying the electronic optical response of molecules in intense fields," *Phys. Chem. Chem. Phys.*, vol. 7, pp. 233–239, 2 2005. DOI: 10.1039/B415849K. [Online]. Available: http://dx.doi.org/10.1039/B415849K.

[9] P.-O. Löwdin, "On the nonorthogonality problem.," in ser. Advances in Quantum Chemistry, P.-O. Löwdin, Ed., vol. 5, Academic Press, 1970, pp. 185–199. DOI: https://doi.org/10.1016/S0065-3276(08)60339-1. [Online]. Available: https://www.sciencedirect.com/science/article/pii/S0065327608603391.

[10] M. Burkatzki, C. Filippi, and M. Dolg, "Energy-consistent pseudopotentials for quantum Monte Carlo calculations," *The Journal of Chemical Physics*, vol. 126, no. 23, p. 234 105, Jun. 2007, ISSN: 0021-9606. DOI: 10.1063/1.2741534. eprint: https://pubs.aip.org/aip/jcp/article-pdf/doi/10.1063/1.2741534/13304179/234105_1_online.pdf. [Online]. Available: https://doi.org/10.1063/1.2741534.

[11] T. Dunning, "Gaussian basis sets for use in correlated molecular calculations. i. the atoms boron through neon and hydrogen," *The Journal of Chemical Physics*, vol. 90, p. 1007, Jan. 1989. DOI: 10.1063/1.456153.

[12] Q. Sun, T. C. Berkelbach, N. S. Blunt, *et al.*, "Pyscf: The python-based simulations of chemistry framework," *WIREs Computational Molecular Science*, vol. 8, no. 1, e1340, 2018. DOI: https://doi.org/10.1002/wcms.1340. eprint: https://wires.onlinelibrary.wiley.com/doi/pdf/10.1002/wcms.1340. [Online]. Available: https://wires.onlinelibrary.wiley.com/doi/abs/10.1002/wcms.1340.

[13] L. Zhao, Z. Tao, F. Pavošević, A. Wildman, S. Hammes-Schiffer, and X. Li, "Real-time time-dependent nuclear–electronic orbital approach: Dynamics beyond the born–oppenheimer approximation," *The Journal of Physical Chemistry Letters*, vol. 11, no. 10, pp. 4052–4058, May 21, 2020. DOI: 10.1021/acs.jpclett.0c00701. [Online]. Available: https://doi.org/10.1021/acs.jpclett.0c00701.

Eidgenössische Technische Hochschule Zürich
Swiss Federal Institute of Technology Zurich

Declaration of originality

The signed declaration of originality is a component of every written paper or thesis authored during the course of studies. In consultation with the supervisor, one of the following three options must be selected:

- (●) I confirm that I authored the work in question independently and in my own words, i.e. that no one helped me to author it. Suggestions from the supervisor regarding language and content are excepted. I used no generative artificial intelligence technologies[1].
- ( ) I confirm that I authored the work in question independently and in my own words, i.e. that no one helped me to author it. Suggestions from the supervisor regarding language and content are excepted. I used and cited generative artificial intelligence technologies[2].
- ( ) I confirm that I authored the work in question independently and in my own words, i.e. that no one helped me to author it. Suggestions from the supervisor regarding language and content are excepted. I used generative artificial intelligence technologies[3]. In consultation with the supervisor, I did not cite them.

Title of paper or thesis:

Extending RT-TDHF to Include Magnetic Field Interactions

Authored by:
If the work was compiled in a group, the names of all authors are required.

Last name(s):	**First name(s):**
Solinas	Massimo

With my signature I confirm the following:
- I have adhered to the rules set out in the Citation Guide.
- I have documented all methods, data and processes truthfully and fully.
- I have mentioned all persons who were significant facilitators of the work.

I am aware that the work may be screened electronically for originality.

Place, date	**Signature(s)**
Zurich, 20/05/2024	Massimo Solinas

If the work was compiled in a group, the names of all authors are required. Through their signatures they vouch jointly for the entire content of the written work.

[1] E.g. ChatGPT, DALL E 2, Google Bard
[2] E.g. ChatGPT, DALL E 2, Google Bard
[3] E.g. ChatGPT, DALL E 2, Google Bard